Vietnam Journal of Mechanics, Vol. 46, No. 4 (2024), pp. 298 – 310
DOI: https://doi.org/10.15625/0866-7136/20660

DEVELOPMENT OF A BATHYMETRY MAP OF THE NHAT LE ESTUARY, QUANG BINH PROVINCE BY REMOTE SENSING TECHNIQUES

Le Thi Huong*, Le Thi Hong Van, Nguyen Thi Viet Lien, Trinh Thi Thu Thuy, Le Nhu Nga, Dang Song Ha
Institute of Mechanics, VAST, 18 Hoang Quoc Viet, Hanoi, Vietnam
*E-mail: lthuong211@gmail.com

Received: 24 April 2024 / Revised: 08 August 2024 / Accepted: 14 August 2024
Published online: 04 September 2024

Abstract. Multispectral remote sensing images with the advantages of low cost, wide area coverage, and increased resolution have been widely used recently for determining the bathymetry of coastal waters. In this study, the correlation equation is developed based on the Landsat 8 OLI satellite images captured on September 22, 2022, and the survey data measured during the time period of September 12–22, 2022, was used for mapping bathymetry in the Nhat Le Estuary area, Quang Binh Province, a relatively clear area from sediment. The correlation between the image and the field survey data is quite good, with R^2 = 0.88. This shows that Landsat 8 OLI data is suitable for mapping sea areas with depths up to 20 m.

Keywords: bathymetry, mapping, satellite image, reflectance spectrum, Landsat 8 OLI image, Nhat Le Estuary.

1. INTRODUCTION

Measurement of ocean bathymetry is typically carried out using echo sounders or Acoustic Wave And Current meter (AWAC), which give pretty accurate results. However, this way of measurement is expensive in cost and requires much time of deployment in practice [1–3].

The Landsat satellite program is developed by the United States Aeronautics and Space Administration (NASA) and the United States Geological Survey (USGS). The first satellite was launched in 1972 and to date, there have been eight generations of satellites developed. Landsat satellite provides data with a resolution range of 15–100 m for

different activities such as monitoring changes in the earth's surface and environmental resources, planning and managing agriculture and urban areas, etc. The Landsat-8 satellite, launched in 2013 has two sensors: OLI (Operational Land Imager) to monitor the surface and TIRS (Thermal Infrared Sensor) to collect thermal infrared images. Landsat 8 OLI provides high/medium spatial resolution imageries with 11 spectral bands, including 9 shortwave bands with a resolution of 15–30 m and 2 longwave thermal bands with a resolution of 100 m.

Light Detection And Ranging (LIDAR) is an active remote sensing technology that uses lasers to survey objects from space. The data obtained by the system based on LIDAR is a collection of 3-dimensional reflection point clouds of laser beams from the object being surveyed on the ground. Digital aerial scanning technology is another method deployed for depth estimation, which is cost-effective compared to monitoring from ships, while providing faster coverage of large areas [4,5]. Over the years, several optical satellite images have been used in many studies to extract depth data. The multispectral sensors can be used to provide a wide range of wavelengths, especially the green and blue bands that can penetrate to depths of 20 m below the sea surface in clear water conditions [6].

As remote sensing data sources with high/medium spatial resolution and open source, which have attracted the great attention from researchers, over decades, Landsat7 ETM+ and Landsat8 LDCM satellites images have been used to estimate bathymetry for coastal areas globally.

The most common algorithms used in these studies are log linear [7,8] and non-linear models [9]. For example, a nonlinear algorithm has been applied to Landsat images in the Wadden Sea region of the Netherlands [10] with a coefficient of determination (R^2) of 0.85 and root square error (RMSE) of 3.12 m; on Thousand Island [11] with R^2 = 0.90 and RMSE = 0.86 m for depths up to 10 m and at the coastal area of Dakshina Kanada in India, Kastela Bay in the middle of the Adriatic Sea with R^2 of 0.90 [12].

Around the world, methods using satellite images to estimate water depth can be divided into two types based on (i) the influence of depth measurement on the propagation and dispersion of surface waves (wave kinematics) and (ii) the relationship between water depth and the penetration and reflection of light in the water (watercolor). Methods based on the radiative transmission of light in water as a function of depth and wavelength (i.e., color-based methods) can be used to estimate depth in optically shallow water [13–19].

In Vietnam, some studies determining depth based on remote sensing data have acknowledged a linear relationship between spectral values and the sea's depth. Specifically, Phan Quoc Yen in 2017 used Landsat 8 OLI data to estimate the depth of shallow

water areas along Truong Sa Island, and the results show that the maximum water depth achieved is 12 m; The correlation coefficient of model R^2 is 0.924; RMSE is 0.99 m [20]. Do Xuan Tinh's research used Sentinel-2 multispectral satellite images and seabed topographic survey data in June 2019 in the Tien Chau estuary area, Phu Yen province, to build a correlation equation to estimate depth, achieved quite good accuracy (correlation coefficient R^2 = 0.7) [21]. Duong Van Phong used Landsat 8 OLI images to evaluate the change in coastal topography in the Da Nang Port area with chart number I-200-32 published in 2011 and carried out by The Surveying and Mapping Team of the Naval Force; this study has determined a fairly high R^2 correlation coefficient of 0.94 [22].

Today, with the development of satellite technology, remote sensing can be considered an effective solution to solve the field survey problems because of its wide area coverage, low cost, short revisit, and high spatial/spectral resolution [23]. This article again presents the ability of remote sensing satellite images for sea depth mapping in terms of and/or new creation and/or updating.

2. STUDY AREA, RESEARCH METHOD, AND DATA USED IN THE STUDY

2.1. Study area

Nhat Le River Mouth is located in Dong Hoi City, Quang Binh Province (Fig. 1), with geographical coordinates 17°29′ North latitude and 106°38′ East longitude. It is the mouth of the Kien Giang River which has a basin of 2,650 km^2 belonging to the lowland area of the Central Coastal Region. In recent years, the river mouth has been deposited with the development of a sandbar on the right side, that makes it difficult for waterway traffic and flood drainage and causes coastal erosion at the left side, influencing the coastal economic and civil works of Dong Hoi City [24]. Therefore, building bathymetry maps for different time periods to find the rule of deposition and erosion in this area is of great scientific and practical significance.

2.2. Research method

2.2.1. *Procedure for determining depth data*

The Landsat image is pretreated to neglect the irrelevant factors and the surface reflectance is determined for calculating the initial depth from the image. The regression process is then carried out for the data calculated from the image and field measurement data to select the optimal regression function, from which the final depth data are determined, and the bathymetry map developed. The error of the final depth data is assessed by the root square error. The procedure of depth data determination by remote sensing image is presented in Fig. 2.

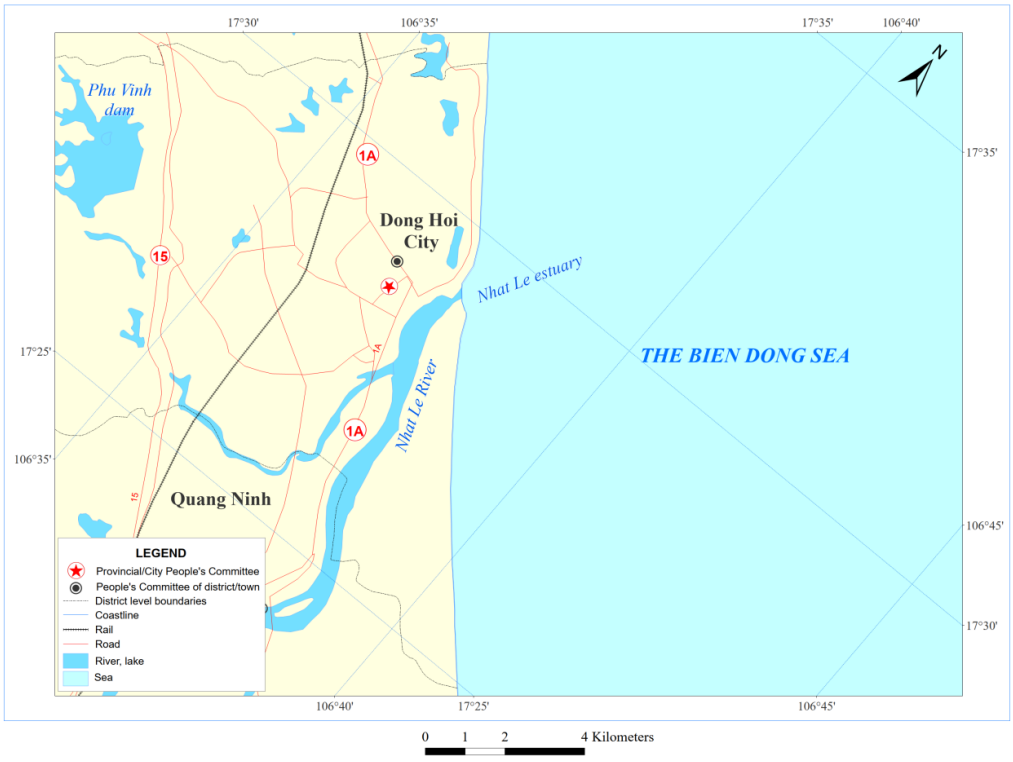

Fig. 1. The study area: Nhat Le Estuary, Quang Binh Province

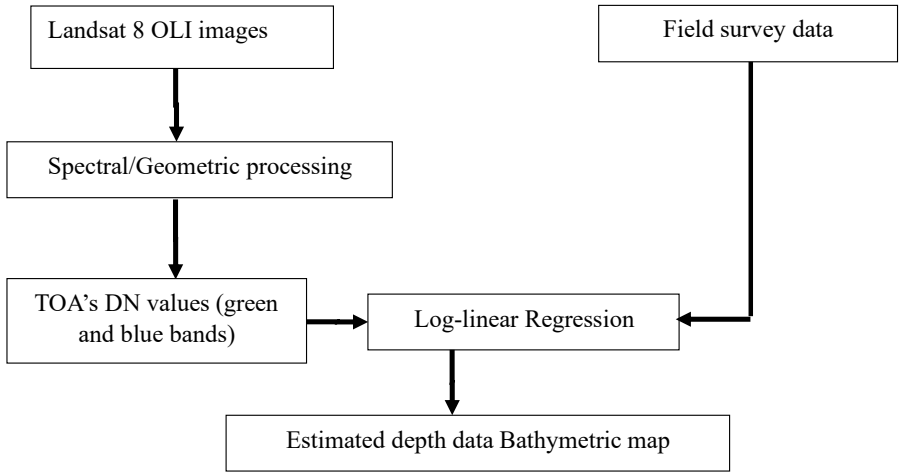

Fig. 2. Flowchart of the study

2.2.2. *Converting gray level values to radiance and reflectance values of objects*

The digital value (DN - Digital Number) on the image is converted to the value of physical radiation at the sensor and the value of physical radiation at the sensor is converted to the value of reflection in the upper atmosphere of the object.

In the first step, the numerical value of the image (corresponding to the gray level) is converted to a physical radiation value. With Landsat 8 OLI images, the radiation value is determined as follows

$$L_\lambda = M_L Q_{cal} + A_L,$$

where L_λ is the TOA spectral radiance; M_L is the band-specific multiplicative rescaling factor from the metadata; (RADIANCE_MULT_BAND_x, where x is the image band number); A_L is the band-specific additive rescaling factor from the metadata (RADIANCE_ADD_L_x and BAND_x, (where x is the image band number); Q_{cal} is the quantized and calibrated standard product pixel value (DN).

The spectral irradiance value obtained in the above step will be used to determine the spectral reflectance value.

For Landsat 8 satellite images, the spectral reflectance value is determined according to the following formula

$$\rho\lambda' = M_p Q_{cal} + A_p,$$

where $\rho\lambda'$ is the TOA planetary reflectance, without correction for solar angle. Note that "$'$" does not contain a correction for the sun angle; M_p is the band-specific multiplicative rescaling factor from the metadata; (REFLECTANCE_MUIL_BAND_x, where x is band number); A_p is the band-specific additive rescaling factor from the metadata (REFLECTANCE_ADD_BAND_x, where x is band number); Q_{cal} is the integer value of the image.

This spectral reflectance value is corrected according to the sun's beam angle according to the following formula:

$$\rho = \frac{\rho'}{\cos(\theta_{SZ})} = \frac{\rho'}{\sin(\theta_{SE})},$$

where ρ is the TOA planetary reflectance; θ_{SE} is the local sun elevation angle. The scene center sun elevation angle in degrees is provided in the metadata (SUN_ELEVATON); θ_{SZ} is the local solar zenith angle: $\theta_{SZ} = 90^\circ - \theta_{SE}$; θ_{SE}, θ_{SZ} taken from the metadata file in the Landsat image data.

2.2.3. *Interpreting coastal water depth using multispectral satellite images*

To obtain bathymetric data from Landsat-8 satellite images, in the study the equation developed by Stumpf and colleagues [9] was applied and a non-linear complex work to estimate depth was performed. By hypothesizing that image channels with higher absorbance will attenuate faster as depth increases, Stumpf and colleagues found that the ratio between the two corresponding image channels will increase as depth increases. Therefore, the ratio between the two image channels will depend on the change in depth rather than on the change in the bottom surface. When taking the ratio of two image channels, we have

$$z = m_1 \frac{\ln\left(L_w\left(\text{Band}_i\right)\right)}{\ln\left(L_w\left(\text{Band}_J\right)\right)} + m_0, \tag{1}$$

where m_0, m_1 are the model constants; L_w (Band_i) and L_w (Band_j) correspond to channels i, j, respectively. In this study, channel i corresponds to the blue channel, j corresponds to the green channel.

The values m_0, m_1 are calculated by comparing the value from the algorithm and the depth value taken from the corresponding chart.

After the depth values are calculated, the correlation between the actual measured depth value and the calculated depth index value is analyzed and found, and then the correlation equation to estimate the water depth based on the depth index in the study area is established.

2.3. Data used in the study

2.3.1. *Satellite image data*

In this study, the Landsat-8 satellite image (code 126/48 LC08_L1TP_126048_20220915_20220922_02_T1), taken on September 22, 2022, with a spatial resolution of 30 m, path/row (Source: `https://www.usgs.gov`) was used. Only two channels (blue and green) of the Landsat-8 image were in concern because they have shorter wavelengths, so the electromagnetic waves of these two channels are able to penetrate thicker water layers than other channels. Furthermore, because the green channel (525–600 nm) has a longer wavelength than the blue channel (450–515 nm), the green channel's radiation can be attenuated faster when transmitted through the water medium, which helps us to distinguish the shallowness and depth of the water area (Fig. 3).

2.3.2. *Field survey data*

A data set of 41 depth points measured by the Institute of Mechanics, Vietnam Academy of Science and Technology during the period of September 12–22, 2022 (Fig. 4) was

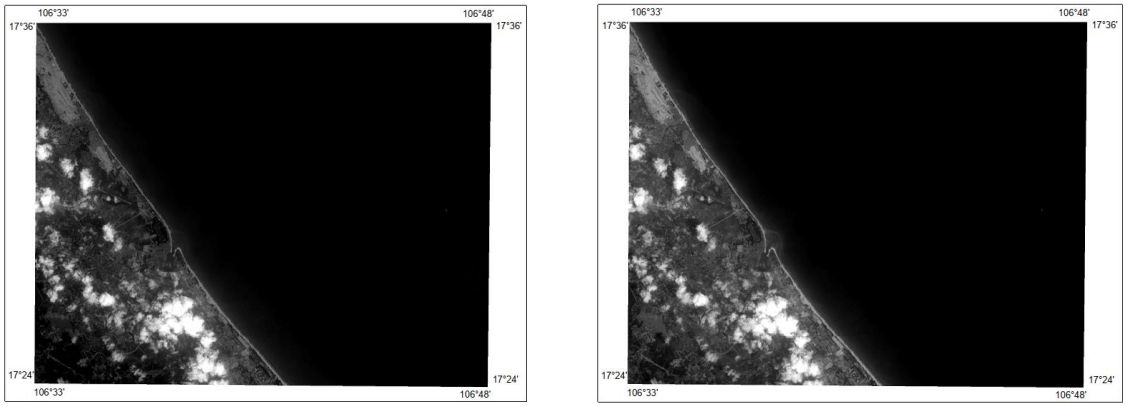

(a) Band 2 (b) Band 3

Fig. 3. Landsat-8 satellite image use in the study

used to determine the constants m, m_1 in the model for calculating depth values from satellite images.

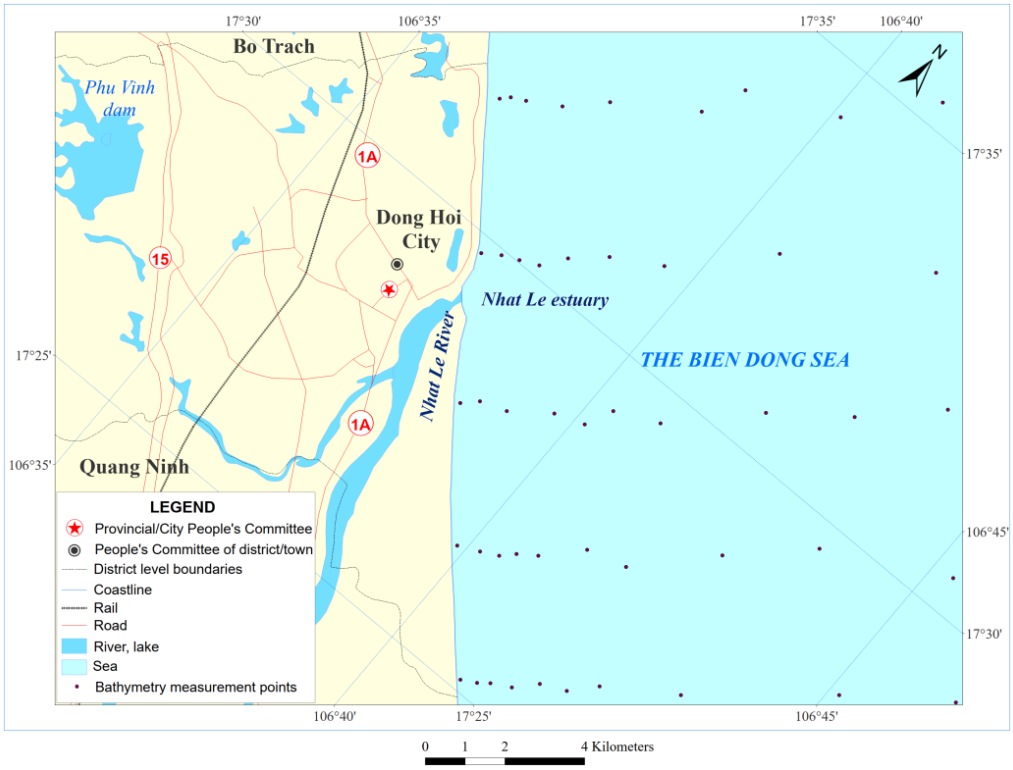

Fig. 4. Depth measurement points outside Nhat Le Estuary

Table 1. Field survey data 41 points

No	Longitude [°]	Latitude [°]	Depth [m]	No	Longitude [°]	Latitude [°]	Depth [m]
1	106.626	17.4962	1.7	22	106.662	17.4790	17.8
2	106.665	17.4419	1.8	23	106.627	17.5411	18.4
3	106.644	17.4672	2.0	24	106.705	17.4326	18.7
4	106.606	17.5254	4.5	25	106.669	17.4815	19.0
5	106.630	17.4988	6.4	26	106.649	17.5141	19.4
6	106.688	17.4210	7.0	27	106.644	17.5527	20.1
7	106.609	17.5275	8.5	28	106.688	17.4601	20.3
8	106.648	17.4703	8.8	29	106.660	17.5205	20.5
9	106.670	17.4443	9.3	30	106.648	17.5628	20.6
10	106.634	17.5006	9.7	31	106.672	17.4880	20.6
11	106.690	17.4229	11.3	32	106.697	17.4628	20.9
12	106.612	17.5292	11.8	33	106.682	17.4927	21.7
13	106.654	17.4725	12.5	34	106.710	17.4382	21.7
14	106.638	17.5025	12.6	35	106.669	17.5719	22.2
15	106.673	17.4463	13.6	36	106.678	17.5394	22.3
16	106.695	17.4252	14.9	37	106.712	17.4787	22.3
17	106.676	17.4491	15.0	38	106.699	17.5098	22.4
18	106.619	17.5335	17.3	39	106.725	17.4485	22.8
19	106.642	17.5079	17.5	40	106.684	17.5893	23.7
20	106.680	17.4520	17.5	41	106.728	17.4940	23.9
21	106.699	17.4299	17.5				

2.3.3. *Topographic map*

The depth contours in the topographic map of Quang Binh Province, scale 1/50,000, were used to verify the model for calculating depth values from satellite images.

3. RESULTS AND DISCUSSION

The constants of the depth calculation model m_1 and m_0 can be calculated by implementing a linear regression algorithm using the actual measured depth values. For each measurement depth point, its corresponding pixel value on the algorithm is collected and calculated. To test the model, the correlation coefficient (R^2), representing the agreement between the measurement depth and the model value was used (Fig. 5). It is necessary to

note that the influence of surface wave is insignificant and already reflected in the correlation coefficient. Fig. 5 shows that the two measured depth values and the model value have a very high correlation with each other (R^2 = 0.86) in the depth range from 1.7 to 23.9 m.

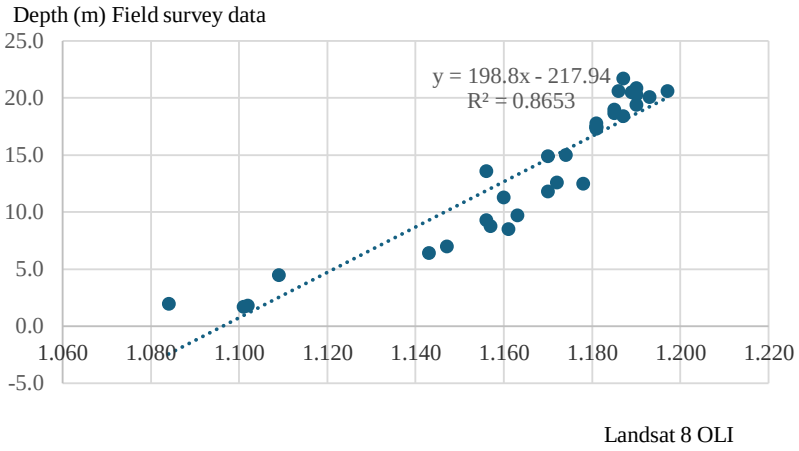

Fig. 5. Correlation chart

The depth result is calculated by taking the ratio between the blue and green image channels and using the found coefficients m_1 and m_0 as shown in Fig. 6.

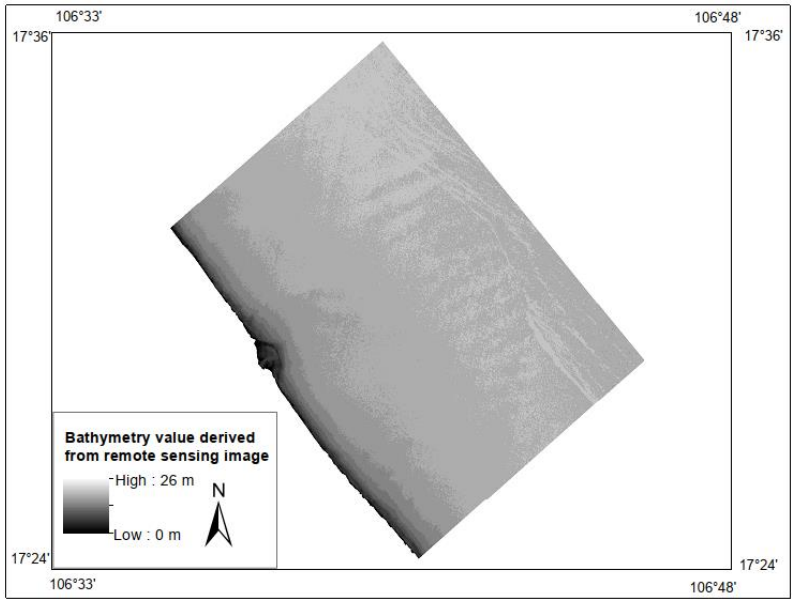

Fig. 6. The processed satellite image (the direct satellite image after computation before editing to become this map)

In addition, to check the accuracy of the study's results, the squared error, another statistical index, was used. Here, the squared error is quite large, RMSE = 2.33 m. The reason is that the Landsat 8 OLI data is saturated at about 20 m.

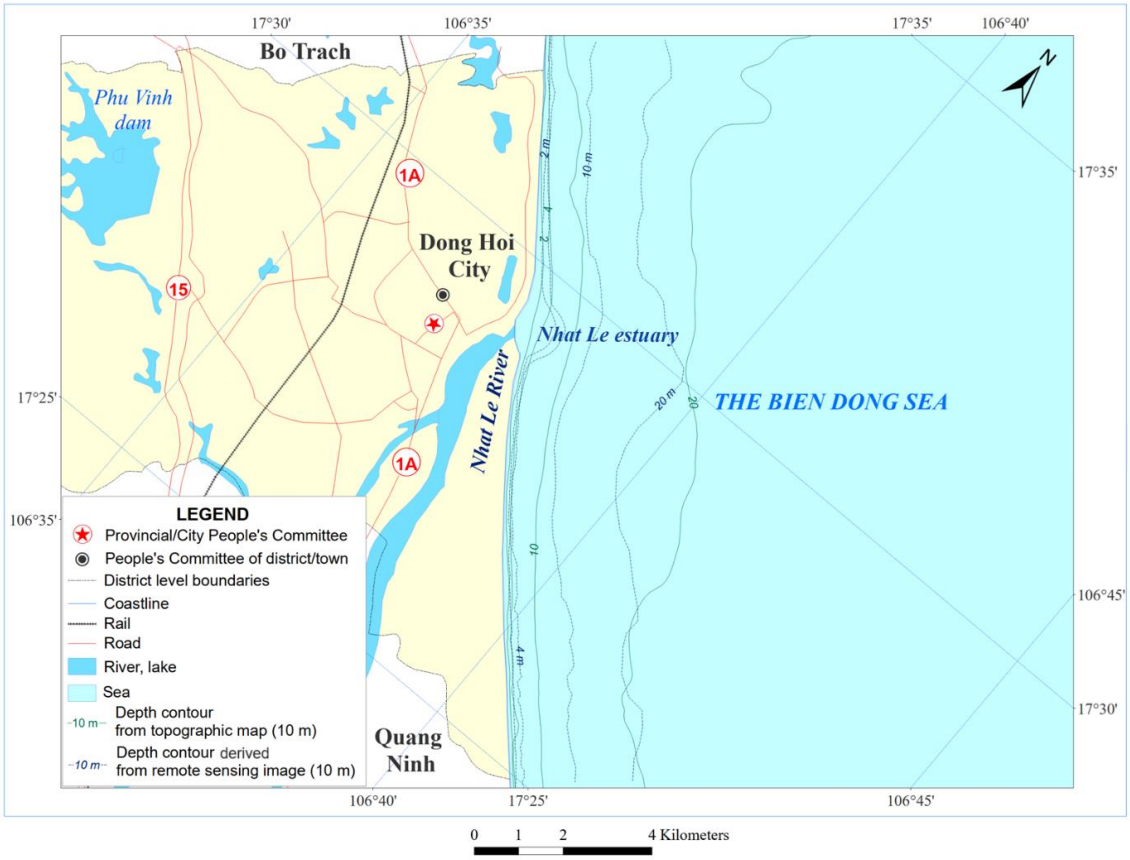

Fig. 7. Comparison of depth contour derived from remote sensing image with topographic map

Furthermore, the depth contours derived from the remote sensing image are quite fitted with the data from the topographic map of Quang Binh Province, scale 1/50,000 (Fig. 7). It means that in this case, the depth model is suitable, reliable, and can be used to determine the depth at the Nhat Le river mouth.

Finally, the bathymetric map of Nhat Le Estuary, Quang Binh Province derived from a remote sensing image is shown in Fig. 8.

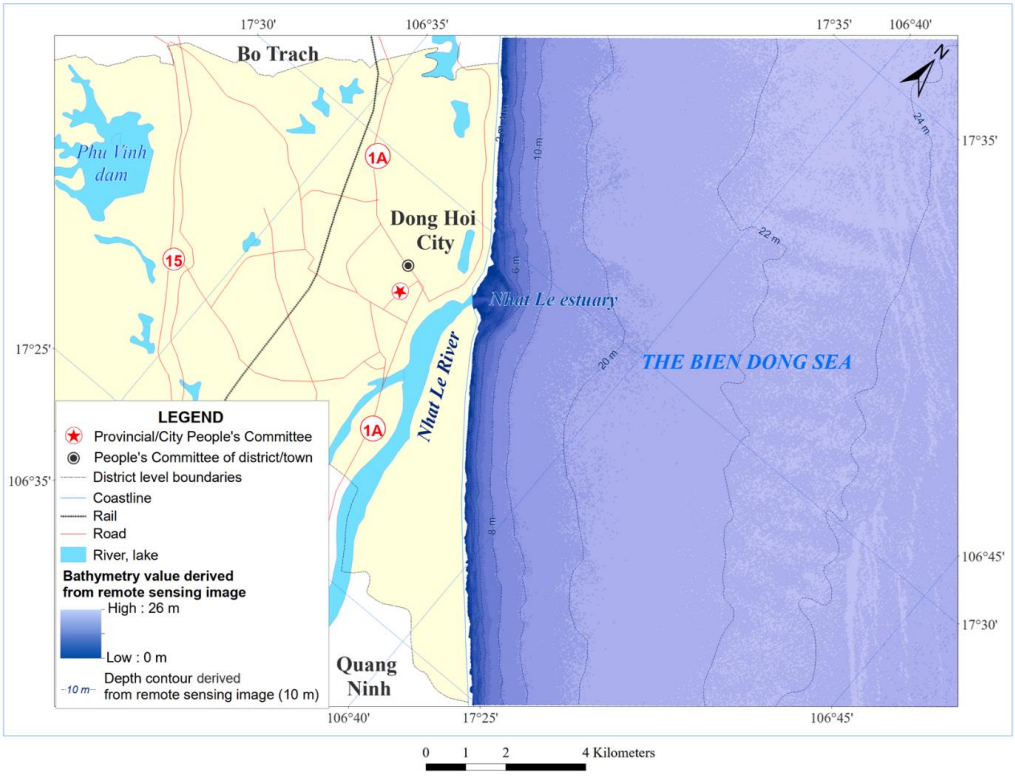

Fig. 8. The bathymetry map of the Nhat Le Estuary, Quang Binh Province derived from remote sensing image

4. CONCLUSION

The results obtained in the study show that determining depth from remote sensing images is a useful tool to build bathymetry maps in shallow water areas instead of traditional depth measurement methods. In addition to building bathymetry maps, this method helps update depth effectively and can be used for reference before deciding to conduct measurements using other depth measurement methods. Currently, Quang Binh Province prioritizes the strong development of the marine economy, especially the coastal urban areas and berths around Nhat Le Port, Gianh Port, and Hon La Port, etc. So, it is important to check for updating the coastal water depth data in the areas and the use of remote sensing images to do it is very reliable.

DECLARATION OF COMPETING INTEREST

The authors declare that they have no known competing financial interests or personal relationships that could have appeared to influence the work reported in this paper.

ACKNOWLEDGMENT

The authors would like to thank the Vietnam Academy of Science and Technology (VAST) for its financial support to the Project "Detailed investigation of marine depth, hydrodynamics and environment of Quang Binh Province", No. CT0000.04/21-22.

REFERENCES

[1] T. A. Kearns and J. Breman. Bathymetry-The art and science of seafloor modeling for modern applications. *Ocean Globe*, **2010**, (2010), pp. 1–36.

[2] E. K. Mccaffrey. A review of the bathymetric swath survey system. *The International Hydrographic Review*, (1981).

[3] N. Sánchez-Carnero, S. Aceña, D. Rodríguez-Pérez, E. Couñago, P. Fraile, and J. Freire. Fast and low-cost method for VBES bathymetry generation in coastal areas. *Estuarine, Coastal and Shelf Science*, **114**, (2012), pp. 175–182. https://doi.org/10.1016/j.ecss.2012.08.018.

[4] J. L. Irish and W. J. Lillycrop. Scanning laser mapping of the coastal zone: the SHOALS system. *ISPRS Journal of Photogrammetry and Remote Sensing*, **54**, (1999), pp. 123–129. https://doi.org/10.1016/s0924-2716(99)00003-9.

[5] H. Ogawa, K. Oyakawa, K. Kawai, H. Ozawa, H. Yajima, H. Shirane, H. Yamano, N. Hirata, N. Iwamoto, and T. Ono. Airborne lidar bathymetry. *Int. Hydrographic Bureau*, (2017), pp. 39–48.

[6] Sutanto. *Penginderaan Jauh Jilid*. Gadjah Mada Press, Yogyakarta, (1992).

[7] D. R. Lyzenga. Passive remote sensing techniques for mapping water depth and bottom features. *Applied Optics*, **17**, (1978). https://doi.org/10.1364/ao.17.000379.

[8] D. R. Lyzenga. Remote sensing of bottom reflectance and water attenuation parameters in shallow water using aircraft and Landsat data. *International Journal of Remote Sensing*, **2**, (1981), pp. 71–82. https://doi.org/10.1080/01431168108948342.

[9] R. P. Stumpf, K. Holderied, and M. Sinclair. Determination of water depth with high-resolution satellite imagery over variable bottom types. *Limnology and Oceanography*, **48**, (2003), pp. 547–556. https://doi.org/10.4319/lo.2003.48.1_part_2.0547.

[10] A. Misra, Z. Vojinovic, B. Ramakrishnan, A. Luijendijk, and R. Ranasinghe. Shallow water bathymetry mapping using Support Vector Machine (SVM) technique and multispectral imagery. *International Journal of Remote Sensing*, **39**, (2018), pp. 4431–4450. https://doi.org/10.1080/01431161.2017.1421796.

[11] J. Pushparaj and A. V. Hegde. Estimation of bathymetry along the coast of Mangaluru using Landsat-8 imagery. *The International Journal of Ocean and Climate Systems*, **8**, (2017), pp. 71–83. https://doi.org/10.1177/1759313116679672.

[12] I. E. Setiawan, D. M. Yuwono, V. P. Siregar, and G. H. Pramono. The study of sea bottom morphology and bathymetric mapping using worldview-2 imagery. In *Seminar Proceeding*, Citeseer, (2013), pp. 143–149.

[13] X. Li and M. C. J. Damen. Coastline change detection with satellite remote sensing for environmental management of the Pearl River Estuary, China. *Journal of Marine Systems*, **82**, (2010), pp. S54–S61. https://doi.org/10.1016/j.jmarsys.2010.02.005.

[14] S. Toure, O. Diop, K. Kpalma, and A. S. Maiga. Shoreline detection using optical remote sensing: A review. *ISPRS International Journal of Geo-Information*, **8**, (2019). https://doi.org/10.3390/ijgi8020075.

[15] I. Caballero and R. P. Stumpf. Retrieval of nearshore bathymetry from Sentinel-2A and 2B satellites in South Florida coastal waters. *Estuarine, Coastal and Shelf Science*, **226**, (2019). https://doi.org/10.1016/j.ecss.2019.106277.

[16] T. Sagawa, Y. Yamashita, T. Okumura, and T. Yamanokuchi. Satellite derived bathymetry using machine learning and multi-temporal satellite images. *Remote Sensing*, **11**, (2019). https://doi.org/10.3390/rs11101155.

[17] E. Evagorou, C. Mettas, A. Agapiou, K. Themistocleous, and D. Hadjimitsis. Bathymetric maps from multi-temporal analysis of Sentinel-2 data: the case study of Limassol, Cyprus. *Advances in Geosciences*, **45**, (2019), pp. 397–407. https://doi.org/10.5194/adgeo-45-397-2019.

[18] C. Giardino, G. Candiani, M. Bresciani, Z. Lee, S. Gagliano, and M. Pepe. BOMBER: A tool for estimating water quality and bottom properties from remote sensing images. *Computers & Geosciences*, **45**, (2012), pp. 313–318. https://doi.org/10.1016/j.cageo.2011.11.022.

[19] C. J. Legleiter, D. A. Roberts, and R. L. Lawrence. Spectrally based remote sensing of river bathymetry. *Earth Surface Processes and Landforms*, **34**, (2009), pp. 1039–1059. https://doi.org/10.1002/esp.1787.

[20] P. Q. Yen, D. K. Hoai, and D. T. B. Hoa. Research Bathymetry Mapping of Shallow Water Areas around Islands in the Truong Sa Archipelago by Deep - Remote sensing technology. *VNU Journal of Science: Earth and Environmental Sciences*, **33**, (2017). https://doi.org/10.25073/2588-1094/vnuees.4194.

[21] D. X. Tinh, T. T. Tung, and T. D. Hung. Analysis of coastal seabed topography changes in Tien Chau estuary, Phu Yen province using Sentinel-2 images. *Hydrometeorological Journal*, **760**, (2024).

[22] D. V. Phong. *Research on the application of satellite images to supplement and update depth charts in Vietnam's coastal waters*, (2022).

[23] P. Jagalingam, B. J. Akshaya, and A. V. Hegde. Bathymetry mapping using Landsat 8 satellite imagery. *Procedia Engineering*, **116**, (2015), pp. 560–566. https://doi.org/10.1016/j.proeng.2015.08.326.

[24] N. T. Hung, V. D. Cuong, and N. V. Hung. Research on seasonal fluctuations of hydrodynamic regime in Nhat Le estuary area, Quang Binh province. *Journal Science and Technology Water Resources*, **48**, (2018).